INVESTIGATION OF LOCALIZED DAMAGE INDICATORS OF A CARBON SHORT-FIBRE REINFORCED HIGH PERFORMANCE CONCRETE UNDER DYNAMIC AND FLEXURAL LOAD

Philipp Lauff [1], Manuel Raith[2], Christian Große[2,] Matthias Rutzen[3], Dirk Volkmer[3], Lisa Reischmann[4], Ursula Weiß[4], Malte A. Peter[4] and Oliver Fischer[1]

[1] Chair of Concrete and Masonry Structures, Technical University of Munich, Germany
[2] Chair of Non-destructive Testing, Technical University of Munich, Germany
[3] Chair of Solid State and Materials Chemistry, University of Augsburg, Germany
[4] Research Unit Applied Analysis, University of Augsburg, Germany

Corresponding author email: oliver.fischer@tum.de, grosse@tum.de; dirk.volkmer@physik.uni-augsburg.de, malte.peter@math.uni-augsburg.de

Abstract

By using a novel fibre-reinforced cement paste recipe in an additive manufacturing ('3D-printing') method, a highly anisotropic material with vastly improved flexural and tensile strength can be created. Extruding the paste through a small nozzle results in unidirectional fibre orientation. A fibre content of 3 vol% results in static flexural strengths of above 100 MPa. High-strength fibre reinforced materials have great potential to be used as small, lightweight construction elements. Those structural members often show susceptibility to oscillating dynamic loads. Using a dynamic-mechanical analyser, miniature samples with a cross-section of 3 mm x 3 mm can be tested for their resistance towards cyclic loading in tests of up to 10 million cycles. Using an ex-situ method, micro-CT scans and optical microscopy are used to check for cracking and other damage indicators.

To investigate the tensile fatigue behaviour on macro scale, bone-shaped specimens under pulsating tensile stress with a cross section area of 50 mm x 50 mm are examined. In addition to standard methods, i.e. strain gauges, strain sensors and position sensors, modern and wide range methods like fibre optic sensors, photogrammetry (digital image correlation), acoustic emission analysis and ultrasonic based coda wave interferometry are used. The aim is to describe the local macro crack development.

The experimental investigations are accompanied by a multiscale modelling approach incorporating three-dimensional representative volume elements based on micro-CT scans of small test specimens. The representative volume elements reflect the mesoscale in the sense that carbon fibres and otherwise homogenized concrete matrix are distinguished.

Keywords: Carbon fibre reinforced concrete, fatigue, 3D-printing, fibre orientation, high tensile strength, multiscale modelling and simulation

1. Introduction

Cementitious materials are well-known to possess high compressive but relatively poor flexural and tensile strength. A way to solve this problem is by reinforcing the cement matrix with materials possessing high flexural strength. Traditionally, this is done using reinforcing steel, however recent studies show great potential in reinforcement with chopped carbon fibres. Using an additive manufacturing ('3D-printing') method, a relatively homogenous but also highly anisotropic material can be created (Hambach & Volkmer 2017). By extruding the paste through a small nozzle, the resulting fibre orientation is mainly unidirectional in the nozzle's movement direction. A content of 3 percent by volume of oriented fibres results in a static flexural strength of above 100 MPa (Hambach et al. 2016). Following this process, the nozzle path can be adjusted beforehand to match an expected

stress profile in the finished structural member. Figure 1 shows a schematic of the process, as well as typical stress-strain diagrams of small 3-point bending beams reinforced with various amounts of carbon fibres, aligned in the direction of the tensile stress occurring during testing.
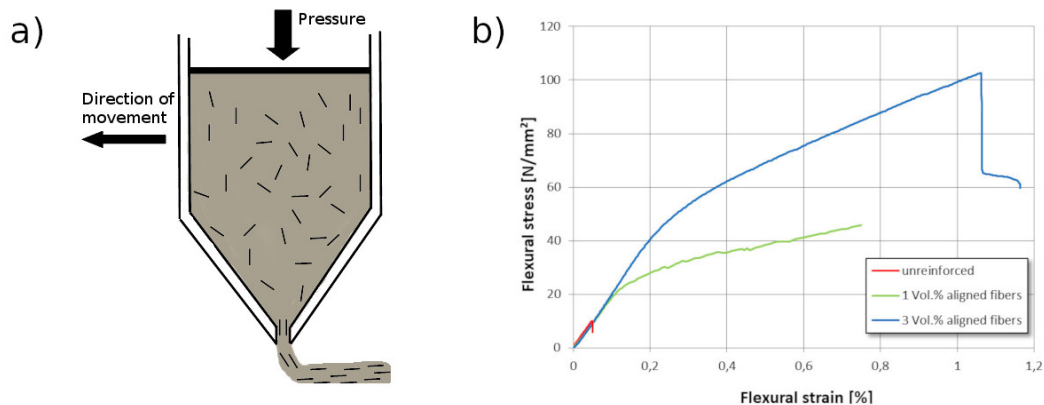

Figure 1. a) Schematic showing the principle behind the nozzle alignment process. As the fibres are extruded through the tight nozzle, they are oriented in the direction of its movement. b) Stress-strain behaviour of unreinforced and fibre-reinforced beam samples in a 3-point bending test.

As can be seen, even relatively small amounts of correctly aligned fibres lead to a sharp increase in ultimate flexural strength and toughness. Characteristically, the samples behave linear-elastically at the beginning of the test, but enter a strain-hardening regime as stress increases and first cracks appear in the matrix. Such behaviour is explained by the formation of multiple micro-cracks which are bridged by the fibres until total fracture (Kanada & Li 1998; Jun & Mechtcherine 2010). A visualization of this can be seen in Figure 2, where the microscopic cracks are made visible via capillary suction by immersing the sample in water for a short time.

Figure 2. Side-view on a miniature beam specimen after being loaded with enough force to undergo micro-cracking during strain-hardening. Micro-cracks are made visible by short immersion in water.

The formation of these micro cracks is a highly localized straining process, which is not adequately described as integral strain of a macroscopic sample. Instead, various measuring techniques (nano-CT, digital microscopy, strain gauges, photogrammetry, acoustic emission analysis etc.) are combined to allow an accurate assessment of these localized phenomena.

While these statements also hold true for static loading experiments, the following research work ultimately wants to explore the influence of carbon fibre reinforcement on cyclic loading. As structural members with fibre reinforcement have great potential to be used as lightweight elements with minimal wall thickness, susceptibility to damage by oscillating forces increases – thus, gaining understanding into the particular mechanisms of these processes is critical.

Conforming to the interdisciplinary idea of an experimental-virtual lab, the insights gathered during the experiments are used for a multiscale modelling approach, which combines a description of a macroscopic workpiece with that of fine structures on the mesoscale with the help of representative volume elements (RVE).

2. Cracking in miniature beam-shaped specimens under static and cyclic flexural load

2.1. Sample preparation

The experiments were carried out using a fibre-reinforced cement paste recipe described by Hambach & Volkmer (2016). A dry mix of 61,5 wt% Portland Cement 52,5 R (Schwenk Zement KG) and

21 wt% silica fume EFACO (Egyptian Ferro Alloys Company SAE) was mixed with 15 wt% of deionized water and 2.5 wt% water reducing agent Glenium ACE 430 (BASF SE) using a Heidolph rotary mixer at 540 rpm. After the cement paste is properly homogenized in the mixing process, the carbon fibres are added (Toho Tenax J HT C261, mean length: 3 mm, mean diameter 7 μm, tensile strength: 3950 MPa, Young's modulus: 230 GPa) and mixed at 60 rpm until they are fully dispersed in the cement paste.

The cement is then filled into a 20 mL plastic syringe (B. Braun-Melsungen AG) and extruded into a PTFE mould of 60 mm x 13 mm x 3 mm. The samples were stored at 100% relative humidity for 24 h for hardening. After this period, they were transferred into a bath filled with deionized water for 6 days and finally stored for another 21 days at 60% relative humidity. After 7 days of storage, the specimens were cut into beams of 60 mm x 3 mm x 3 mm using a Buehler IsoMet low-speed saw.

2.2. Investigation of fracture zones using CT

As a first step, the material's behaviour under static flexural load is investigated. A beam-shaped sample with dimensions of 60 mm x 3 mm x 3 mm was loaded in a 3-point bending setup until failure using a Zwick/Roell Zwicki-Line Z0.5 Universal Testing Machine with 5 kN load cell attached. After failure, the zone next to the fatal macroscopic crack was investigated for damage by CT-scan.

The small cross-section of 3 mm x 3 mm allows the samples to be examined via x-ray CT with high resolution and no further sample preparation. Using a GE nanotom m CT-scanner, voxel sizes between 1.5 μm and 2 μm were typically achieved. One scan comprises 2500 single pictures taken with a voltage of 190 kV and a current of 70 μA. Reconstructions were carried out using the software phoenix datos|x, ring-shaped artefacts were removed automatically during post-processing. The reconstructed images were viewed and processed in VGStudio Max 2.1. Figure 3 shows a CT-scan of a beam sample after static failure in a 3-point bending test. Greyscale values that correspond with fibres are marked in red.
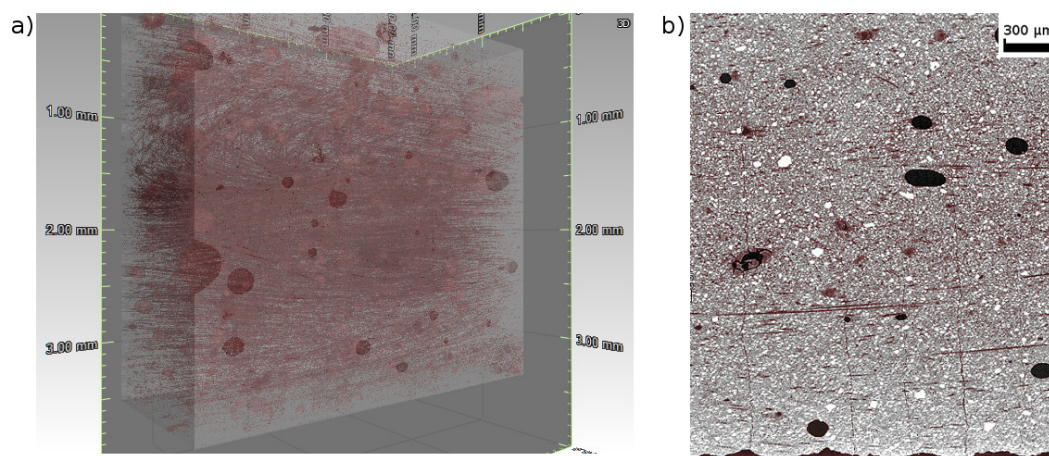

Figure 3. Reconstructed CT-scan of a fibre-reinforced sample after a static 3-point bending test. Greyscale values corresponding to fibres and voids are marked in red. a) Transparent 3D reconstruction of the whole scan showing fibres and voids as red isosurface b) Region of interest from a tomographic slice showing cracks advancing from the bottom of the sample.

As can be seen in Figure 3b, fibres, cracks and pores are visible to the human eye; however, the segmentation is accompanied by huge amounts of noise. The greyscale values of carbon fibres and those of voids and minor inclusions in the matrix are within a very narrow range, so separation between these elements is not possible with a simple greyscale value selection process. Current investigations are underway to find post-segmentation algorithms to filter out the noise. These are based on geometrical parameters, to allow for proper quantitative analysis of strength defining characteristics of the sample.

Once the segmentation optimization procedure is finished, samples will be investigated for damage caused by cyclic load in an ex-situ method. A sample is put under cyclic load using a TA Instruments Q800 Dynamic-Mechanical Analyser. After a certain number of load cycles it is scanned using X-Ray CT. Once the scan is complete, the sample undergoes a cyclic loading regime again and the process is

repeated until the sample fails. This way, the growth of specific single cracks in the scanned area should be possible. This information then allows conclusions to be drawn regarding the mechanisms behind crack propagation in fibre-reinforced cementitious composites.

2.3. CT scans as basis for the construction of an RVE

In addition to microstructural analysis, the CT data is meant to serve as a basis for multiscale numerical modelling. To allow the influence of small particles like carbon fibres to be properly shown in a simulated macroscopic workpiece, the use of representative volume elements (RVE) is necessary. To allow for easier segmentation, carbon fibres with a wider diameter (Kreca Chop C-103 T, Kureha GmbH, mean diameter: 16.3 µm, mean length: 3.1 mm, tensile strength: 875 MPa, Young's modulus: 35 GPa) were used. The reconstructed scan can be seen in Figure 4.
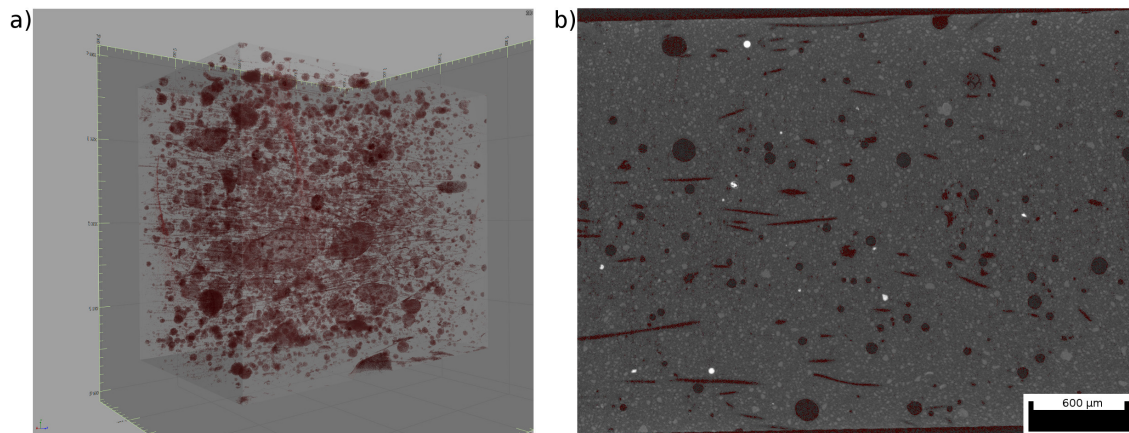

Figure 4. Reconstructed CT-scan of a sample containing carbon fibres with a diameter of 16.3 µm, serving as a basis for RVEs. Greyscale values corresponding with fibres and voids are marked in red. a) Transparent 3D reconstruction of the whole scan showing fibres and voids as red isosurface. b) Tomographic slice showing segmented fibres and voids marked in red.

As Figure 4 shows, there is much less noise included in the final segmentation due to the coarser nature of the fibres. While the fibres are not suitable for improving the mechanical properties of the composite due to low modulus and strength, they provide a valuable starting point in the creation of an RVE for modelling purposes, since factors like fibre alignment angles have not visibly changed while the quality of the segmentation is much better.

3. Cracking in macroscale bone-shaped specimens under static and cyclic uniaxial tension

For the production of larger test specimens, a 3D printer was developed, which enables a precise positioning of the extruded strands and ensuring the fibre orientation. For pumping concrete, different pumping methods were investigated, as special demands were placed on the pumping system due to high viscosity and strong cross-sectional taper of the nozzle. Another necessary feature is a fast response time to track speed changes so that too much or too little material is extruded during acceleration and deceleration ramps. Finally, the best results could be achieved with an air-pressure-controlled piston pump which compresses a foil cartridge. The extruded strands are accurately placed next to each other using the 3D printer to avoid unwanted macro pores between the strands.

There are many different possibilities to adjust the path of the nozzle. As shown in Figure 5, the circular outlines of the specimen require a similar path to assure a smooth distribution of forces and to avoid staircase shaped outlines. Especially during fatigue testing, erratic changes in cross section can lead to stress peaks and early specimen failure. Therefore, different nozzle paths were constructed and examined in terms of homogenous matrix and few macro pores in between printed strands.
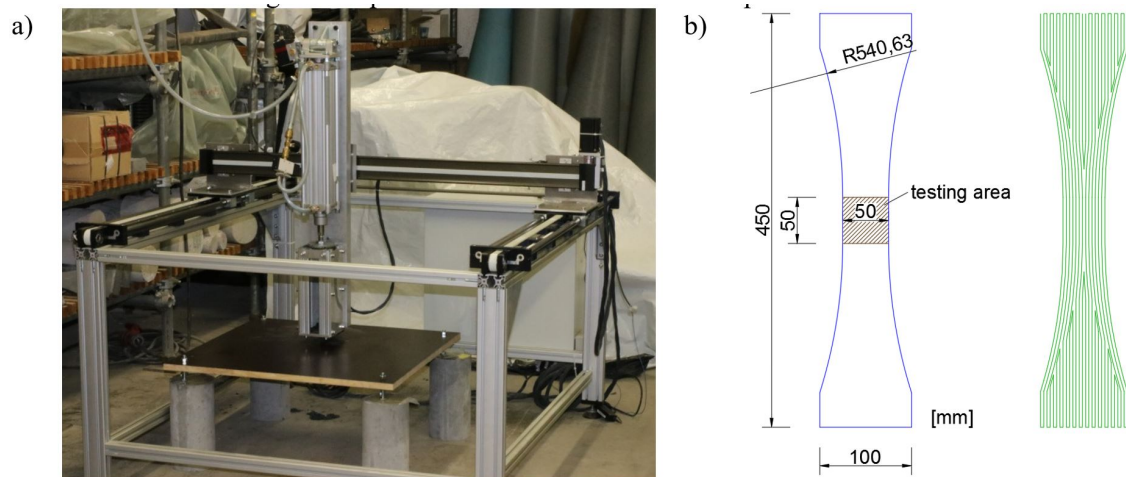
Figure 5. 3D concrete printer for the production of tensile specimen (a), their dimensions and the used nozzle path (b)

Next to the specimen shown in Figure 5, there will be tests on smaller ones which are also bone-shaped but only 160 mm in length to investigate the influence of size. During the whole research project, different carbon fibre contents, swinging speeds and load levels from 20 to 80% with a bottom to top load ratio of 20% of short term resistance will be applied. One of the project's main aspects is to examine the behaviour in construction-practical stress levels and to determine the residual capacities after previous high-cyclic loading. For this purpose, Wöhler tests in the cracking phases II and III will be discontinued on the basis of the observed damage and the remaining loadbearing capacity will be determined. With this information, we hope to be able to infer from the transition of phases I/II to the resistance of total number of cycles.

The tensile static and dynamic test will be carried out with clamped ends of the specimen. Due to the concrete behaviour of cracking, the real cross section is diminished mostly eccentric. While using a loose jointed connection, there will be a repositioning of the specimen in the way that the reduced cross section will be loaded centrically. Based on the primary and non-cracked profile, there is a bending load which cannot be determined in dimension by the strain measurement. Therefore the specimen is glued with duromer adhesive MC-Bauchemie MC-DUR 1280 to the bearing plates connected to the servo-hydraulic testing machine EVO 1000.

Another aim to achieve within this research project is to observe closely the crack process while working with non-notched specimens. Therefore it is necessary to use wide range measurement equipment like fibre optical sensors, photogrammetry, acoustic emission analysis and ultrasonic based coda wave interferometry.

In the fibre optic measurement, glass fibres are glued on the specimen surface and scanned at short intervals using a laser beam. Internal mismatches, density and geometry variations in the glass fibre reflect parts of the laser beam (Rayleigh backscatter). The strain change of the glass fibre causes a wavelength change of the light. This makes it possible to determine the actual change in strain within the glass fibre. The distance of individual measuring points is only a few millimetres, so that a very detailed statement of the strain profile in the direction of the glass fibre can be determined, as shown in Figure 6. (Schmidt-Thrö, Scheufler & Fischer (2016))

The photogrammetry is based on the observation of the surface deformation by means of two cameras (stereo camera). With these, it is possible to detect a very precise pixel shift in space at a low camera–object distance in order to calculate the strains on the specimen's surface (see Figure 6). In addition, this measurement method operates without contact, which means that no faulty measurements through the connection (adhesive) can occur.
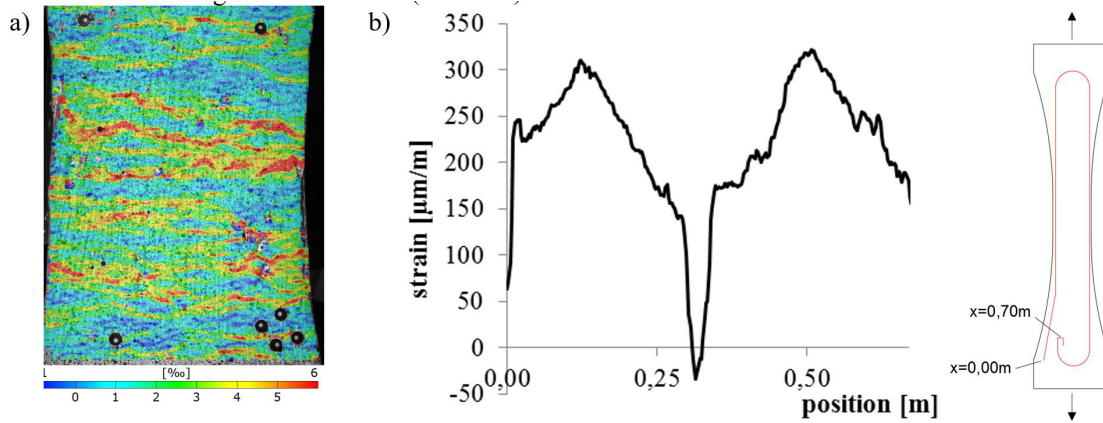
Figure 6. Microcrack analysis with surface strain measurement, i.e. photogrammetry (a) and fibre optical sensor (b)

In addition to the methods of near-surface strain measurement, methods that provide information about the entire sample volume are very useful. To begin with, the sound emission analysis should be mentioned. Failure to deform a brittle material beyond the yield point will result in the failure of single components and, similar to earthquakes, this failure will result in the sudden release of energy dissipated in the form of mechanical waves. These mechanical waves can be registered on the surface and thus provide an insight into the underlying damage mechanism. In advance to the acoustic emission experiments, the compressional wave velocity must be determined. Therefore, a scanning ultrasound measurement method, given in Figure 7a was applied on two material samples. A dense spatial sampling of 1 mm yields a compressional wave velocity of $c_p = 4605 \pm 40$ m/s and a surface wave velocity $c_r = 2357 \pm 3$ m/s. The resulting wave-field is shown in Figure 7b). Based on these wave velocities, the dynamic elastic modulus was computed to E = 29,891 ± 450 N/mm².
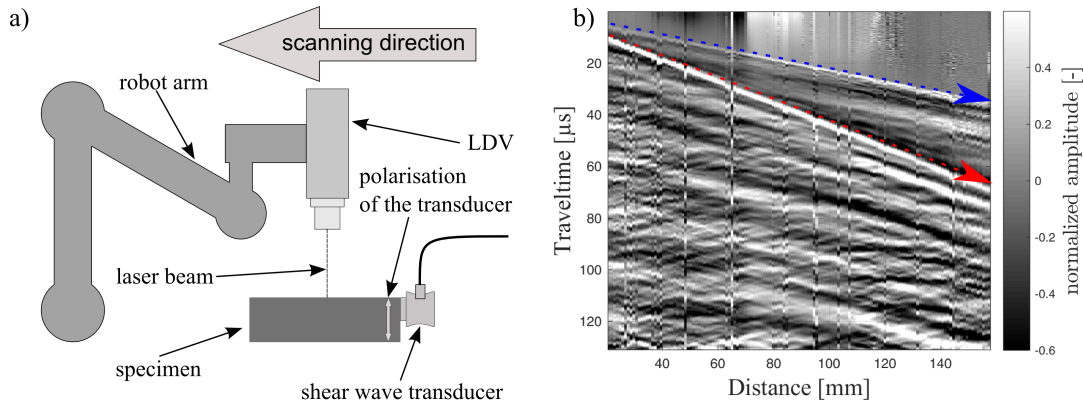

Figure 7 . a) B-Scan measurement setup and resulting image; b) the incident compression wave is highlighted by the blue arrow and the surface wave is indicated by the red arrow.

The modulus of elasticity and wave propagation velocities are sensitive to development of micro-cracks (Thiele 2018). Therefore, future cyclic loading experiments will be monitored using ultrasound transmission measurements in order to capture the development of micro cracks and elastic parameters over time.

4. Multiscale numerical simulation

The numerical simulation of the mechanical behaviour of concrete, which is reinforced by short carbon fibres, requires a multiscale approach taking into account the scale of the carbon fibres besides the specimen scale. Pretests have shown that aggregates and pores do not need to be resolved explicitly for this material. Therefore, in the simulation, we consider the macroscopic workpiece and resolve the carbon-fibre scale by representative volume elements (RVE). The computational-

homogenisation approach (see Zohdi & Wriggers 2005, Charalambabis 2010 or Geers et al. 2010) then requires the determination of the (local) material law in each macroscopic point with the help of the solution of cell problems posed in the RVE at that point. In particular, the macroscopic relation of the deformation gradient ∇u and the stress tensor σ is determined by averages of quantities determined in the RVE leading to a numerical material law of the form

$$\sigma = f\,(\nabla u), \tag{1}$$

where the mapping f resolves the macro–micro–macro transition and represents the local effective material law.

In order to be able to simulate the carbon-fibre-reinforced concrete realistically, the RVEs are taken from μ-CT-data (cf. Section 1.3). For this purpose, the carbon fibres are identified in typical μ-CT-data volume elements. In order to be able to convert these into finite element meshes, the fibre centrelines are marked. After export into the finite element software, they are expanded cylindrically to the diameter of the used carbon fibres. The aspect ratio of the carbon fibres and the fact that they are (more or less) aligned requires the use of long cuboid representative volume elements.

Figure 8 shows a representative volume element of size 950 μm x 950 μm x 3670 μm extracted from μ-CT-data (Figure 8a) and reconstructed in Comsol Multiphysics (Figure 8b) for fibre reinforced UHPC with carbon fibres of 16.3 μm diameter and 3.1 mm length. The number of carbon fibres (whole or parts thereof) contained in the RVE is 130. The full specimen, from which the RVE was extracted, is of size 3.33 mm x 2.44 mm x 3.97 mm and the volume fraction of carbon fibres is 1.08 %. The resolution of the μ-CT-data is given by a voxel side length of 1.67 μm.
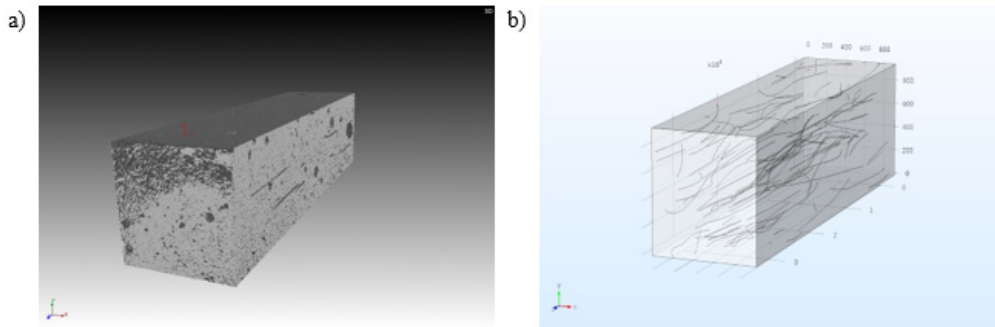

Figure 8 . Representative volume element of size 950 μm x 950 μm x 3670 μm: a) from μ-CT-data, b) reconstructed in Comsol Multiphysics. The single fibres of the RVE, oriented in z-direction, were extracted from μ-CT-data and imported in Comsol Multiphysics via Matlab LiveLink.

Figure 9 shows a cross-section of the RVE depicted in Figure 8 normal to the y-axis of μ-CT-data (Figure 9a) and reconstructed data (Figure 9b). Figure 9a shows a cross-section of the RVE as an image with depth of one voxel. Figure 9b illustrates the same cross section of the reconstructed data. In order to achieve visual comparability, a corresponding slice with depth 33.4 μm (about 20 voxels) is cut out of the reconstructed RVE in Comsol.
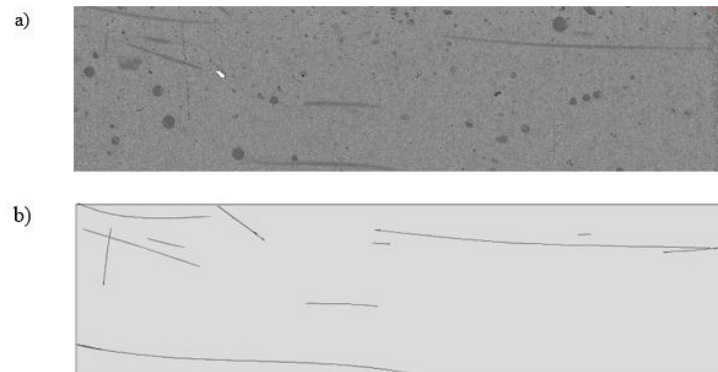

Figure 9. Cross-section of the RVE a) from μ-CT-data and b) reconstructed in Comsol Multiphysics.

Numerical simulations based on this approach and comparisons with experimental data are currently underway. As a future step, it is planned to incorporate cracks on the scale of the carbon fibres as observed in specimens having undergone cyclic loading and comparing the simulated mechanical properties with the experimentally measured data in order to gain a better understanding of the influence of microscopic cracks on the durability of the carbon fibre reinforced UHPC.

5. Conclusions

The use of carbon short fibre reinforced concrete opens up completely new possibilities in terms of economic construction and thin-walled components. However, the associated additional considerations with regard to the fatigue behaviour play a more important role than it is the case with conventional concrete components. The highly effective use of carbon fibres makes it possible to produce a high-performance material that exceeds other cementitious materials in terms of tensile strength by far.

In order to investigate the fatigue behaviour and especially the crack development of this concrete, complex examinations are carried out both on flexural and tensile test specimen. At this point, the CT analysis, large-scale surface strain measurements and acoustic emission analysis are mentioned. The main focus lies on the documentation of crack development and material degradation. The knowledge gained in this way is finally translated into mathematical models to be able to predict the point of failure. Finally, the results are reconciled with measurement data, so that the cycle of the micro–macro–micro relationship is closed.

Acknowledgements

References

Charalambakis, N. (2010): Homogenization Techniques and Micromechanics. Survey and Perspectives; Appl. Mech. Rev. 63

Geers, M.G.D.; Kouznetsova, V.G.; Brekelmans W.A.M. (2010): Multi-scale computational homogenization: trends and challenges; J. Comp. Appl. Math 234, pp. 2175-2182

Hambach, M.; Möller, H.; Neumann, T.; Volkmer, D. (2016): Portland cement paste with aligned carbon fibres exhibiting exceptionally high flexural strength (> 100 MPa); Cement and Concrete Research 89, pp. 80-86

Hambach, M.; Volkmer, D. (2017): Properties of 3D-printed fibre-reinforced Portland cement paste; Cement and Concrete Composites 79, pp. 62-70

Jun, P.; Mechtcherine V. (2010): Behaviour of Strain-hardening Cement-based Composites (SHCC) under monotonic and cyclic tensile loading, Part 1 – Experimental Investigations; Cement & Concrete Composites 32, pp. 801-809

Kanada T., Li V.C.(1998); Multiple Cracking Sequence and Saturation in Fibre Reinforced Cementitious Composites; Concrete Research and Technology 9

Schmidt-Thrö, G.; Scheufler, W.; Fischer, O. (2016): Kontinuierliche faseroptische Dehnungsmessung im Stahlbetonbau. Beton- und Stahlbetonbau, Vol. 111, pp. 496-504

Zohdi, T. I.; Wriggers, P. (2005): An Introduction to Computational Micromechanics, Lecture Notes in Applied and Computational Mechanics, Volume 20, Corrected Second Printing, Springer, ISBN: 978-3-540-77482-2